

Stevin report 25.6.90.05.A1/12.06  
TNO-IBBC report BI-90-049/63.5.3850

FATIGUE STRENGTH OF MULTIPLANAR WELDED HOLLOW SECTION JOINTS AND  
REINFORCEMENT MEASURES FOR REPAIR

THIRD TECHNICAL INTERIM-REPORT (March 1990)

Period 01-07-1989 - 31-12-1989

Contract : - 7210-SA/114  
Mannesmannröhren-Werke A.G. Düsseldorf

Laboratories : - Technische Universität Karlsruhe  
Versuchsanstalt für Stahl, Holz und Steine  
Prof.dr.ir. F. Mang

- Delft University of Technology , Dept of Civil  
Engineering and IBBC-TNO, Rijswijk  
Prof.dr.ir J. Wardenier

Research team : Dr. R.S. Puthli (TNO-IBBC, Rijswijk)  
C.H.M. de Koning (TNO-IBBC, Rijswijk)  
A. Romein (Delft University)  
E. Panjeh. Shahi (Delft University)  
A. Verheul (Delft University)

Prof.dr.ir. J. Wardenier (Delft University)  
(project coordinator for the ECSC sub contract  
in the Netherlands)

Dipl.ing. D. Dutta (Mannesmannröhren-Werke A.G.  
Düsseldorf)  
(Project coordinator for the ECSC contract)

CECA Convention Nr. 7210-SA/114

Investigation with financial aid of the European Community of Steel  
and Coal.

## CONTENTS

1. General introduction
2. Numerical investigation
3. Experimental investigation
  - 3.1 Multiplanar joints in C.H.S
  - 3.2 Multiplanar joints in R.H.S
4. References

Tables

Figures

# FATIGUE STRENGTH OF MULTIPLANAR WELDED HOLLOW SECTION JOINTS AND REINFORCEMENT MEASURES FOR REPAIR

## 1.0 GENERAL INTRODUCTION

This programme deals with the fatigue strength of multiplanar welded hollow section joints and reinforcement measures for repair. The Dutch part consists of the testing of 4 triangular girders made of circular hollow sections (CHS) and 4 triangular girders made of rectangular hollow sections (RHS). All these girders are provided with strain gauges to determine the loading distribution and the hot spot stresses for verification with numerical models. The fatigue tests are used to determine the fatigue lives and to check the results with those obtained for uniplanar joints. After the appearance of certain crack length the cracks are repaired and fatigue testing is continued to check the effectivity of the various repair methods. The final objective is to define design rules in relation to those for uniplanar joints.

This report describes the work carried out at Delft University of Technology and IBBC-TNO in the period 01-07-1989 and 31-12-1989.

Up to the end of 1989 fabrication of the girders was finished and a start was made with the testing one CHS and one RHS girder. Up till now only preliminary results can be given.

Chapter 2 of this interim report give a brief survey of the Numerical investigation work carried out at Delft University.

Chapter 3.1 gives a brief survey of the Experimental investigation of the multiplanar joints in C.H.S carried out at IBBC-TNO.

Chapter 3.2 gives brief survey of the Experimental investigation of the multiplanar joints in R.H.S carried out at Delft University of Technology.

## 2.0 NUMERICAL INVESTIGATION

### 2.1 NUMERICAL MODELLING OF MULTIPLANAR GIRDERS

In the static analysis of multiplanar lattice girders, secondary bending moments can be neglected when determining the load distribution patterns in the girder, provided there is sufficient deformation capacity. The numerical modelling can then be simplified by assuming all members to be pin ended.

However, the influence of bending moments, including secondary bending, become important for fatigue analysis. This is because axial loads as well as bending moments affect the hot-spot stresses at the joints. Any influence, therefore, on the hot-spot stress range affects fatigue life.

All eight girders to be investigated (four in CHS and four in RHS) in this programme contain 14 joints (figure 2.1), of which 4 joints are being studied for stress concentration factors.

In order to get a realistic load distribution, the complete girder could be modelled with a combination of beam and shell elements.

This would mean that the girder contains a large number of nodes and elements, so that very large computer storage would be required to analyse such a model.

It is anticipated that for a reasonable accuracy in the calculation of the stiffness properties of an isolated multiplanar KK-joint, about 1000 elements are needed.

This means that for the analysis of one girder, there are a total of about 14000 elements needed, which requires extremely large computer storage capacities and can become very expensive to analyse.

The simple solution to this problem is to model the whole girder with beam elements, with the physical properties of the elements at the joints so modified that behaviour of the girder modelled numerically is the same as the girder being loaded (figure 2.2).

The fictitious physical properties of the beam elements at the joints can be determined from comparison with the behaviour of an isolated joint made of shell elements under applied load, using a finite element program.

For a beam element:

$$[K] * \{\delta\} = \{P\} \quad \text{where} \quad [K] = \text{stiffness matrix}$$

(As defined in figure 2.3)

$$\{\delta\} = \text{displacement vector}$$
$$\{P\} = \text{load vector}$$

Using the applied loads and corresponding deflections of the modelled joint in the above formula, the fictitious physical properties of each beam element can be obtained (figure 2.4).

The calculated properties are then used in modelling the girder made of beam elements.

The girder modelled with the modified physical properties can then be analysed to obtain the loads and bending moments.

These can be compared with the results obtained from the experimental investigation on test girders.

## 2.2 COMPUTER FACILITIES.

I-DEAS is used for pre- and post processing.

Model Solution of I-DEAS and DIANA are used for finite element analysis.

I-DEAS pre-processing is divided into two parts namely:

- Geomod;
- Supertab.

In Geomode solid modeling of the joint is carried out. Figures 2.5 and 2.6 show some typical solid models prepared in Geomode.

Supertab takes surfaces of solid models made in Geomode and allows nodes and elements to be created on these surfaces.

Figures 2.7 to 2.12 show some examples of the nodes and elements created.

Once the model preparation is complete, restraints, constraints and loads may be applied to the Finite Element model.

The model can then be analysed using a finite element computer program.

The post-processing of Ideas, permits interrogation of calculated results in the form of print out or visual presentation.

### 2.3 SCF CALCULATION.

With the aid of pre-processing in I-DEAS, the finite element model of a joint including the weld geometry made of solid elements will be prepared.

The measured forces at pre-defined locations in the girder are then applied to the isolated joint, to obtain the resulting hot-spot stresses and strains at the critical locations.

These are converted to stress concentration factors and can be directly compared with the experimental investigations.

It is expected that the simulation of this part will be carried out in the second half of 1990.

### 3.1 THE FATIGUE BEHAVIOUR OF MULTIPLANAR JOINTS IN C.H.S

#### 3.1.1 Joints in circular hollow sections

For the experimental investigation 4 girders have been fabricated. A review of the specimens with their identification number is given in table 3.1.1. The configuration and dimensions of these girders are shown in figure 3.1.1. Each girder has two multiplanar gap joints and two multiplanar overlap joints to be investigated, with joint parameters  $\beta = 0.4$  and  $0.6$ ,  $2\gamma = 12$  and  $24$  and a constant thickness ratio  $r = 0.5$ . The material quality of the hollow sections used for the girders is Fe 360.

Girder 5 which is being tested first is fully instrumented with strain gauges in two cross sections of all the members. In this way the axial strains, and the bending strains (bending in plane and bending out of plane) can be measured at a static loading.

Also, strain strips have been applied in a number of crown- and saddle points of the main joints to determine the strain distribution in these locations. From this the hot spot strain at the weld toes can be determined by means of linear extrapolation, figure 3.1.2 shows a detail of an instrumented gap joint.

The measured dimensions and the material properties ( $\sigma_{e_0}$ ,  $\sigma_{u_0}$ ,  $\epsilon$ ) of the hollow sections used for girder 5 have also been determined.

The test rig for the girders in C.H.S. is shown in figure 3.1.3 and 3.1.4. For girder 5, the first measurements at static loading have been carried out. Fatigue testing starts at the beginning of 1990.

It is expected that the tests on girder 5, the analysis of the results and the comparison with the numerical work will be finished in the beginning of the second quarter of 1990.

In the mean time, girder 6 will be instrumented with strain gauges and can be tested directly after girder 5.

## 3.2 THE FATIGUE BEHAVIOUR OF MULTIPLANAR JOINTS IN R.H.S

### 3.2.1 Introduction.

This part of the programme deals with the experimental investigation of 4 specimens of multiplanar joints in R.H.S

A review of the specimens with their identification number is given in table 3.2.1. The configuration and dimensions of the specimens are given in figure 2.1. Each girder has two multiplanar gap joints and two multiplanar overlap joints to be investigated, with joint parameters  $\beta = 0.4$  and  $0.6$ ,  $2\gamma = 12.5$  and  $25$  and a constant thickness ratio  $\tau = 0.5$ . Figure 3.2.1 shows the testrig for the specimen (multiplanar joints in R.H.S).

In this period the experimental investigation of Girder 2 has been started.

### 3.2.2 Measured dimensions and mechanical properties

The rectangular hollow sections of girder 2 are hot finished with steel grade Fe 360 for the section  $200 \times 200 \times 16$  and Fe 430 for the sections  $80 \times 80 \times 8$ , according to Euronorm 25-72.

The measured dimensions and actual mechanical properties are given in table 3.2.2 whereas the joint parameters are given in table 3.2.3.

The yield stresses  $f_y$  of all segments were determined with stub column tests. The stub columns had lengths of  $2.5 b$ .

The ultimate stress and the permanent elongation were determined with tensile tests (dp 5) and were carried out in accordance with Euronorm 2-57.

### 3.2.3 Test procedure

Before fatigue testing specimen Girder 2 was statically loaded. The static load was increased by small steps up to the maximum load of the required dynamic load range for fatigue testing. After this loading procedure the load was decreased in steps to zero. During this test procedure strain gauge measurements were carried out after each loading step. From these measurements the possible non-linearity between load and strain caused due to the residual stresses can be determined. After 10

cycles the procedure was repeated. The strain measurements from the static test after 10 cycles show a linear relationship with the loading for all strain gauges.

After the static test procedure the fatigue test was carried out to determine the number of cycles to crack initiation and complete failure. A constant amplitude loading with a frequency of 1 Hz and R= 0.1 was applied. During the test the load level was maintained by a loading control unit, which was connected to the hydraulic system of the jack.

#### 3.2.4 Strain distribution.

To determine the axial load and bending moments in the members of Girder 2 all the braces were provided with strain gauges in two cross sections (see Fig. 3.2.2). In the chords CA and CB, two cross section were provided with two strain gauges between each joint. In the chord CC each section between the joints, was provided with four strain gauges in two cross sections .

For determination of the strain distribution in the joints various corners were provided with strain strips on the chord as well as on the brace as shown in figure 3.2.3 to 3.2.6.

#### 3.2.5 Test results

The first test results of girder 2 are given in table 3.2.4. The nominal strain ranges in the braces are determined as follows:

$$\epsilon_{r_{nom}} = \epsilon_{r_{ax}} + \epsilon_{r_{IPB}} + \epsilon_{r_{OPB}}$$

The values under consideration are extrapolated according to figure 3.2.7. The results of the extrapolation of the nominal strain gauges are presented graphically in the figures 3.2.8 and 3.2.9.

In these figures the axial load, IPB moments as well as the OPB moments are expressed in microstrain.

The  $\epsilon_{r_{hs}}$  given in table 3.2.4 has been determined by quadratic extrapolation as given in figure 3.2.10 whereas the SNCF is defined as:

$$SNCF = \epsilon_{r_{hs}} / \epsilon_{r_{nom}}$$

### 3.2.6 Modes of failure.

Member brace A of gap joint ABCD (see fig. 3.2.11) failed in the tension chord at 126.000 cycles.

The crack initiated in corner 4, location A4-D of brace A at the weld toe of the chord. The crack developed along the weld toe perpendicular to the chord axis.

At 90.000 cycles the crack had grown around corner 3 and at 126.000 cycles the crack had grown through the wall of the chord.

The crack of brace A after failure is shown in figure 3.2.12.

The repair method and further failures will be reported in the next interim report.

### 3.2.7 $S_r$ - N diagram.

For comparison with previous investigations [1], the fatigue result of Girder 2 (member A) has been plotted in the  $S_r$  - N diagram presented in figure 3.2.12.

In the diagram it is shown that the fatigue result of member A fit well with the results of the previous test with comparable thicknesses,

The results of the other joints of this girder will be reported in the next interim report.

#### 4. REFERENCES

- [1] Puthli, R.S., Koning, C.M.H. de, Wingerge, A.M. de, Wardenier, J., and Dutta, D.,: "Fatigue strength of welded unstiffened RHS-joints in latticed structures and vierendeel girders"  
Final report - Part III  
TNO-IBBC report BI-89-097/63.5.3820, Stevin report 25-6-89-36/A1  
CECA Convention nr. 7210-SA/111

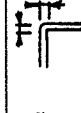
Girder	Nominal dimensions		$\beta$	$2\gamma$	$\tau$	Weld	R-Ratio
	Chord $d_0 * t_0$	Brace $d_1 * t_1$					
5	193.7*8	76.1*4	0.4	24	0.5	fillet	+ 0.1
6	193.7*16	76.1*8		12		butt	
7	193.7*8	114.3*4	0.6	24		fillet	
8	193.7*16	114.3*8		12		butt	

Table 3.1.1 : Review of the specimens in C.H.S.

Girder	Nominal dimensions		$\beta$	$2\gamma$	$\tau$	Weld	R-Ratio
	Chord $b_0 * h_0 * t_0$	Brace $b_1 * h_1 * t_1$					
1	200*200*8	80*80*4	0.4	25	0.5	fillet	+ 0.1
2	200*200*16	80*80*8		12.5		butt	
3	200*200*8	120*120*4	0.6	25		fillet	
4	200*200*16	120*120*8		12.5		butt	

Table 3.2.1 : Review of the specimens in R.H.S.

Table 3.2.2 Measured dimensions and mechanical properties of girder 2 (RHS)

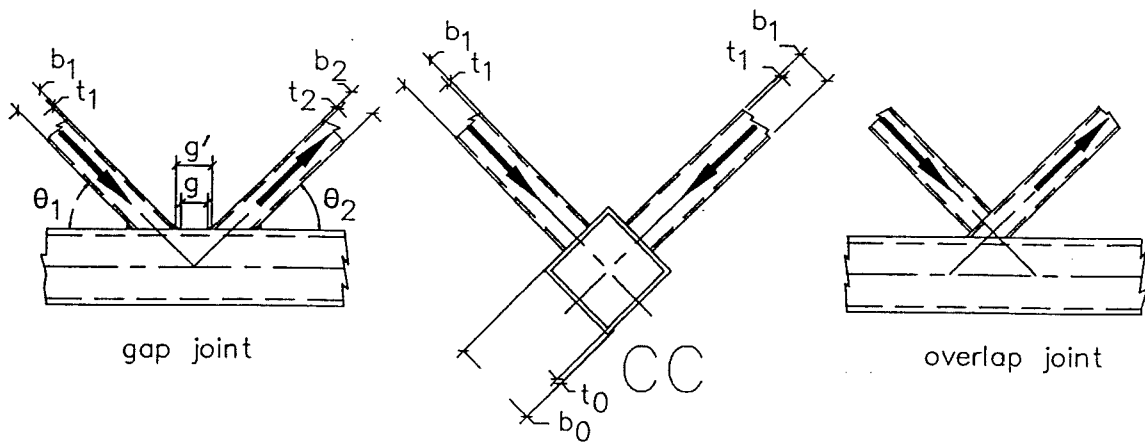
member	location	dimensions (actual) $b_0 * h_0 * t_0$ mm	A (actual) mm <sup>2</sup>	 $t_{0_4}$ mm	 $r_{0_0}$ mm	$f_y^{*)}$ N/mm <sup>2</sup>	$f_u^{**)}$ N/mm <sup>2</sup>	$\epsilon^{**)}$ %	comments
				 $t_{1_3}$	 $r_{1_0}$				
CA	compr. chord	200.7*200.7*15.8	11398	17.9	19.5	236	377	40	
CB	compr. chord	200.5*200.5*15.9	11398	18.2	19.6	243	399	36	
CC	tension chord	200.2*200.2*15.5	11362	17.8	18.7	242	383	35	
A	tension brace	79.7*79.7*7.6	2104	8.6	10.4	285	433	36	
B	tension brace	79.7*79.7*7.6	2101	8.7	10.4	290	432	35	
C	compr. brace	79.7*79.7*7.6	2101	8.7	10.4	290	432	35	
D	compr. brace	79.7*79.7*7.6	2101	8.7	10.4	290	432	35	
E	tension brace	79.7*79.7*7.6	2104	8.6	10.4	285	433	36	
F	tension brace	79.7*79.7*7.6	2101	8.7	10.4	290	432	35	
G	compr. brace	79.7*79.7*7.6	2104	8.6	10.4	285	433	36	
H	compr. brace	79.7*79.7*7.6	2101	8.7	10.4	290	432	35	
I	compr. brace	79.7*79.7*7.6	2104	8.6	10.4	285	433	36	
J	compr. brace	79.7*79.7*7.6	2104	8.6	10.4	285	433	36	
K	tension brace	79.7*79.7*7.6	2101	8.7	10.4	290	432	35	
L	tension brace	79.7*79.7*7.6	2104	8.6	10.4	285	433	36	
M	compr. brace	79.7*79.7*7.6	2104	8.6	10.4	285	433	36	
N	compr. brace	79.7*79.7*7.6	2104	8.6	10.4	285	433	36	
O	tension brace	79.7*79.7*7.6	2101	8.7	10.4	290	432	35	
P	tension brace	79.7*79.7*7.6	2101	8.7	10.4	290	432	35	

\* ) stub column tests

\*\* ) Tensile coupon tests

Table 3.2.3 Joint parameters of girder 2 (RHS) (average value)

joint	$\frac{\beta}{b_1+b_2}$	$\frac{2\gamma}{b_0}$	$\frac{r}{t_1+t_2}$	$\theta_1$	$\theta_2$	g	$g^1$	lap $O_v$ %	ecc e
	$2b_0$	$t_0$	$2t_0$						
A,C-CC	0.398	12.9	0.49	45.5	45	78	68		-4
B,D-CC	0.398	12.9	0.49	45	45	87	83		0
E,G-CC	0.398	12.9	0.49	45	45	87	83		0
F,H-CC	0.398	12.9	0.49	45	45	87	80		0
I,K-CC	0.398	12.9	0.49	45	45			100	-100
J,L-CC	0.398	12.9	0.49	45.5	45			100	-100
M,O-CC	0.398	12.9	0.49	45	45			100	-100
N,P-CC	0.398	12.9	0.49	45.5	45			100	-100



\*\*\*\*\*  
 \*  
 \* Fatigue strength of multiplanar welded square hollow \*  
 \* section joints and reinforcement measures for repair \*  
 \* "Girder 2" \*  
 \*\*\*\*\*

HSSNR and SNCF based on crack location ( quadratically extrapolated )															
Member	Chord	Brace	R	Load range KN	S <sub>r nom</sub> N/mm <sup>2</sup>	ε <sub>r nom</sub> 10 <sup>-6</sup>	ε <sub>r hs</sub> *10 <sup>-6</sup>		SNCF		location		Ni *10 <sup>6</sup>	Nf *10 <sup>6</sup>	Mode of failure
							chord	brace	chord	brace	chord	brace			
A	200*200 t=16	80*80 t=8	0.1	500	136	649	1265	1285	1.95	1.98	A4-D	A4-E	0.055	0.126	CHORD
B					136	649	1168	895	1.80	1.38	B4-D	B4-E	0.055	-	
C					-120	-572	-801	-1155	1.40	2.02	C1-B	C1-A	-	-	
D					-120	-572	-	-	-	-	-	-	-	-	
E					115	550	1276	918	2.32	1.67	E4-D	E3-F	0.064	-	
F					115	550	1276	918	2.23	1.67	) <sup>1</sup>	) <sup>1</sup>	0.064	-	
G					-139	-662	-1059	-1125	1.60	1.70	G1-B	G1-E	-	-	
H					-139	-662	-	-1515	1.66	2.29	H1-B	H1-E	-	-	
I			0.1	500	-167	-795	-397	-1002	-0.50	1.26	I3-D	I4-E	-	-	
J					-167	-795	-365	-	-0.46	-	J3-D	-	-	-	
K					88	421	863	619	2.05	1.47	K4-D	K2-A	-	-	
L					88	421	836	580	2.05	1.38	L4-D	L2-A	-	-	
M					-165	-784	-	-	-	-	-	-	-		
N					-165	-784	-	-	-	-	-	-	-		-
O					177	844	1224	1510	1.45	1.79	O4-D	O1-A	0.055		
P					177	844	1317	—	1.56	-	P4-D	-	0.055		

Ni= crack initiation  
 Nf= end of test (crack through)

$$\epsilon_{r nom} = \epsilon_{r ax} + \epsilon_{r ipb} + \epsilon_{r opb}$$

)<sup>1</sup> no strain gauges available SNCF's used from brace E.

Table 3.2.4 : Test results with quadratically extrapolated HSSNR and SNCF , based on crack location

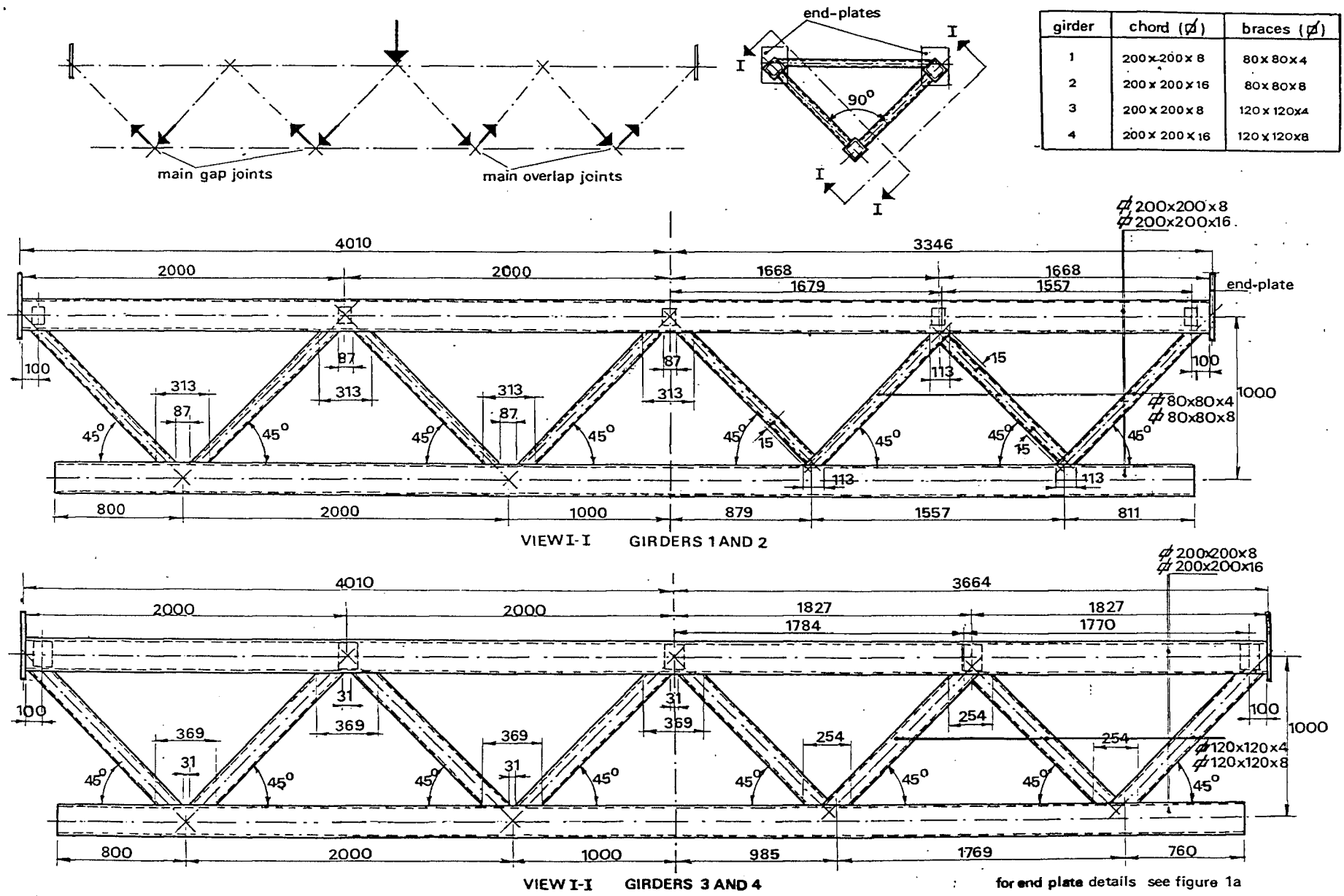
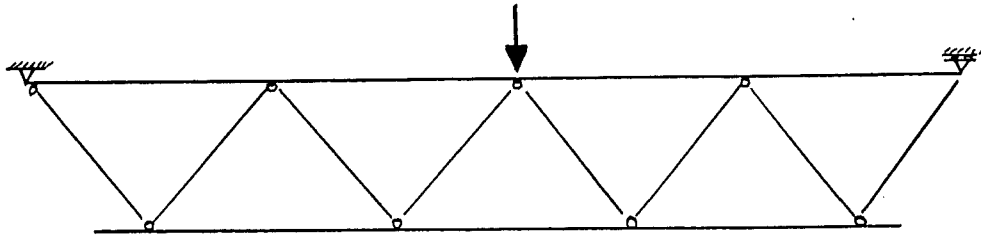
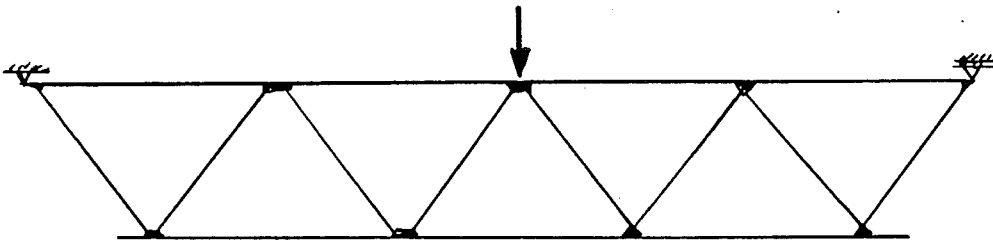


Figure 2.1 Configuration and Dimensions of the Girders in R.H.S.

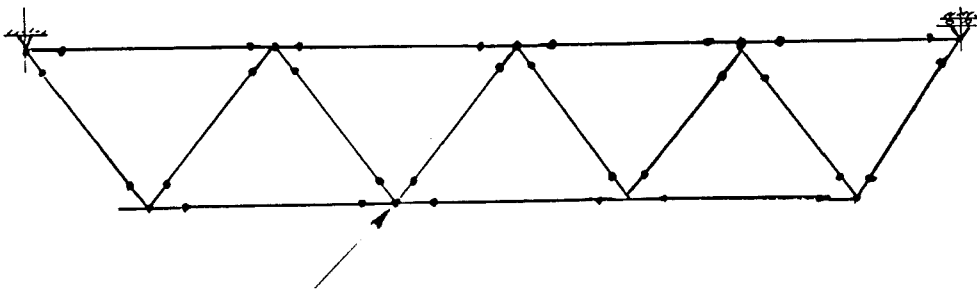
Figure 2.2 Alternative calculation models.



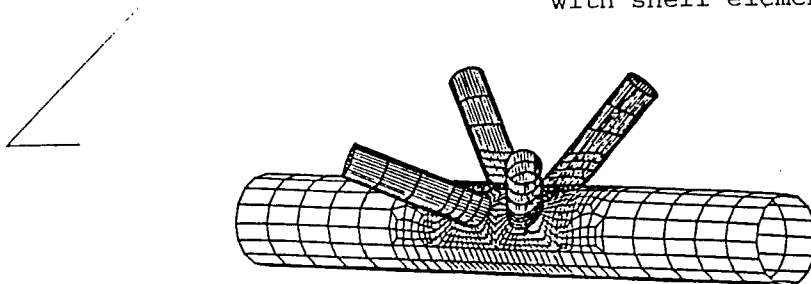
1. Pin ended elements



2. Rigidly jointed elements.



3. Substructuring. (Replacing the beam elements at joints with shell elements).



	EA/L	0	0	0	0	0	-EA/L	0	0	0	0	0
	0	$\lambda_y/L$	0	$-e_z \lambda_y/L$	0	$\frac{1}{2} \lambda_y$	0	$-\lambda_y/L$	0	$e_z \lambda_y/L$	0	$\frac{1}{2} \lambda_y$
	0	0	$\lambda_z/L$	$e_y \lambda_z/L$	$-\frac{1}{2} \lambda_z$	0	0	0	$-\lambda_z/L$	$-e_y \lambda_z/L$	$-\frac{1}{2} \lambda_z$	0
	0	$-e_z \lambda_y/L$	$e_y \lambda_z/L$	$\mu$	$-\frac{1}{2} e_y \lambda_z$	$-\frac{1}{2} e_z \lambda_y$	0	$e_z \lambda_y/L$	$-e_y \lambda_z/L$	$-\mu$	$-\frac{1}{2} e_y \lambda_z$	$-\frac{1}{2} e_z \lambda_y$
	0	0	$-\frac{1}{2} \lambda_z$	$-\frac{1}{2} e_y \lambda_z$	$p_z$	0	0	0	$\frac{1}{2} \lambda_z$	$\frac{1}{2} e_y \lambda_z$	$-q_z$	0
	0	$\frac{1}{2} \lambda_y$	0	$-\frac{1}{2} e_z \lambda_y$	0	$p_y$	0	$-\frac{1}{2} \lambda_y$	0	$\frac{1}{2} e_z \lambda_y$	0	$-q_y$
[K]	-EA/L	0	0	0	0	0	EA/L	0	0	0	0	0
	0	$-\lambda_y/L$	0	$e_z \lambda_y/L$	0	$-\frac{1}{2} \lambda_y$	0	$\lambda_y/L$	0	$-e_z \lambda_y/L$	0	$-\frac{1}{2} \lambda_y$
	0	0	$-\lambda_z/L$	$-e_y \lambda_z/L$	$\frac{1}{2} \lambda_z$	0	0	0	$\lambda_z/L$	$e_y \lambda_z/L$	$\frac{1}{2} \lambda_z$	0
	0	$e_z \lambda_y/L$	$-e_y \lambda_z/L$	$-\mu$	$\frac{1}{2} e_y \lambda_z$	$\frac{1}{2} e_z \lambda_y$	0	$-e_z \lambda_y/L$	$e_y \lambda_z/L$	$\mu$	$\frac{1}{2} e_y \lambda_z$	$\frac{1}{2} e_z \lambda_y$
	0	0	$-\frac{1}{2} \lambda_z$	$-\frac{1}{2} e_y \lambda_z$	$-q_z$	0	0	0	$\frac{1}{2} \lambda_z$	$\frac{1}{2} e_y \lambda_z$	$p_z$	0
	0	$\frac{1}{2} \lambda_y$	0	$-\frac{1}{2} e_z \lambda_y$	0	$-q_y$	0	$-\frac{1}{2} \lambda_y$	0	$\frac{1}{2} e_z \lambda_y$	0	$p_y$

$$\frac{1}{\lambda_y} = \frac{L^2}{12EI_{yy}} + \frac{1}{k_y GA} \quad p_y = \frac{EI_{yy}}{L} + \frac{1}{2} \lambda_y L \quad q_y = \frac{EI_{yy}}{L} - \frac{1}{2} \lambda_y L$$

$$\frac{1}{\lambda_z} = \frac{L^2}{12EI_{zz}} + \frac{1}{k_z GA} \quad p_z = \frac{EI_{zz}}{L} + \frac{1}{2} \lambda_z L \quad q_z = \frac{EI_{zz}}{L} - \frac{1}{2} \lambda_z L$$

$$\mu = (CI_x + \lambda_z e_y^2 + \lambda_y e_z^2)/L$$

Figure 2.3 Stiffness matrix of a 3D beam including forces, shears and moments.

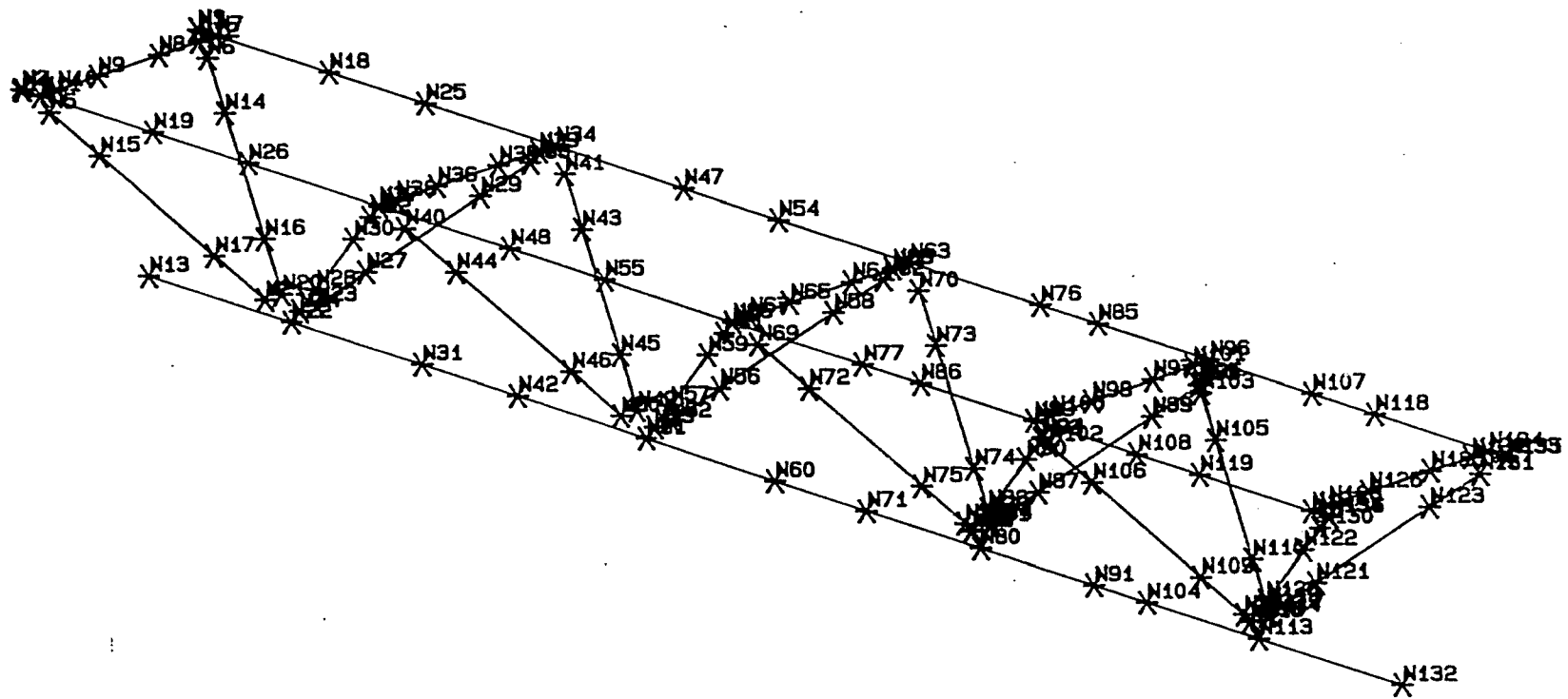
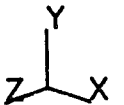


Figure 2.11 Perspective view of a girder made of beam elements.



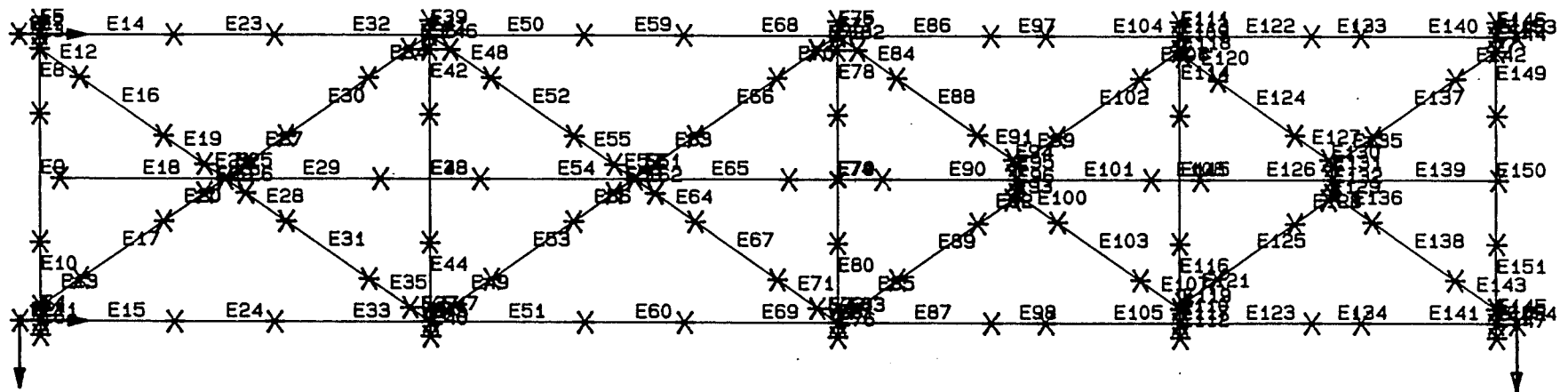


Figure 2.12 Plan view of a girder made of beam elements.



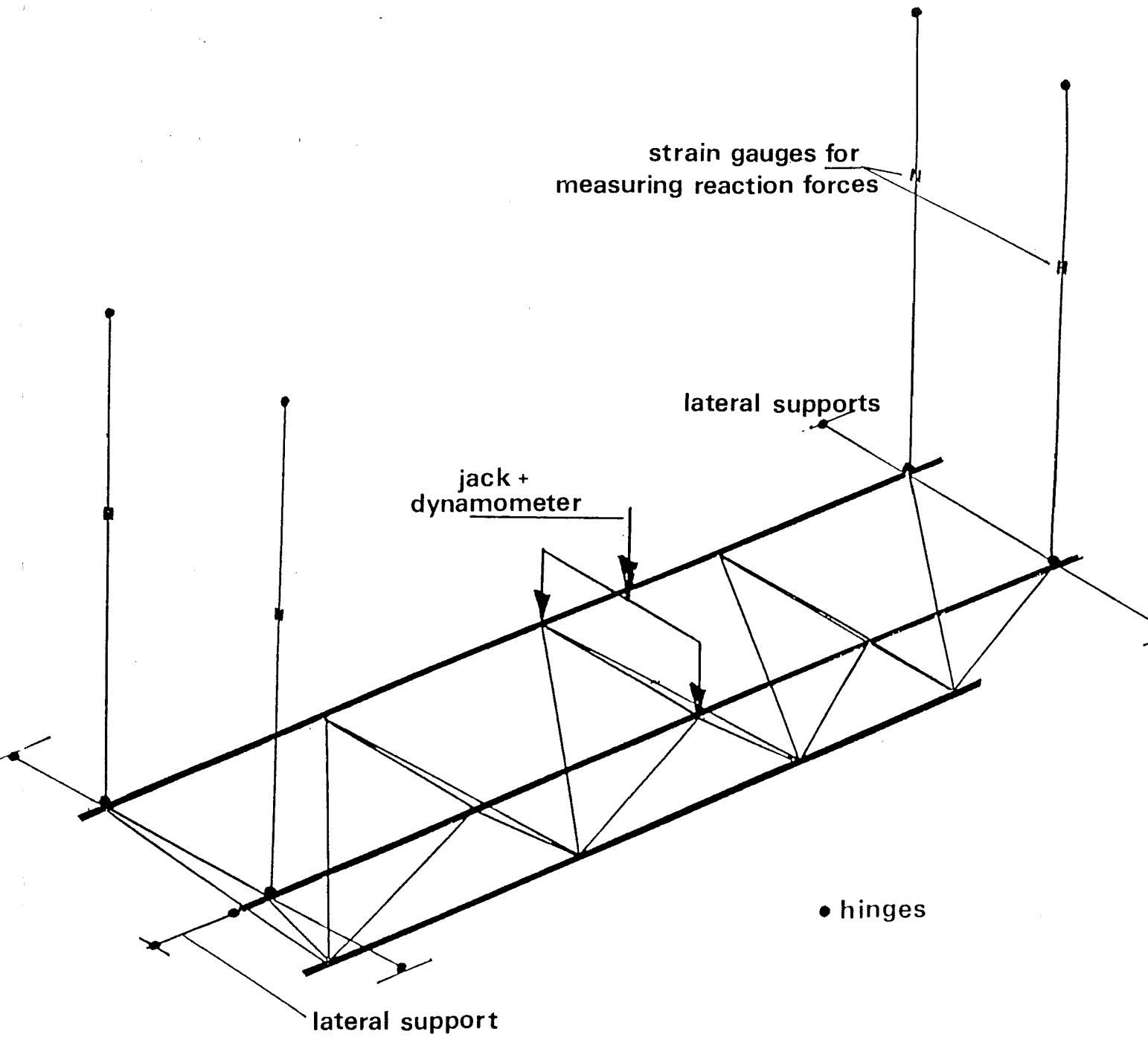


figure 3.1-3 TEST RIG FOR GIRDERS IN C.H.S.

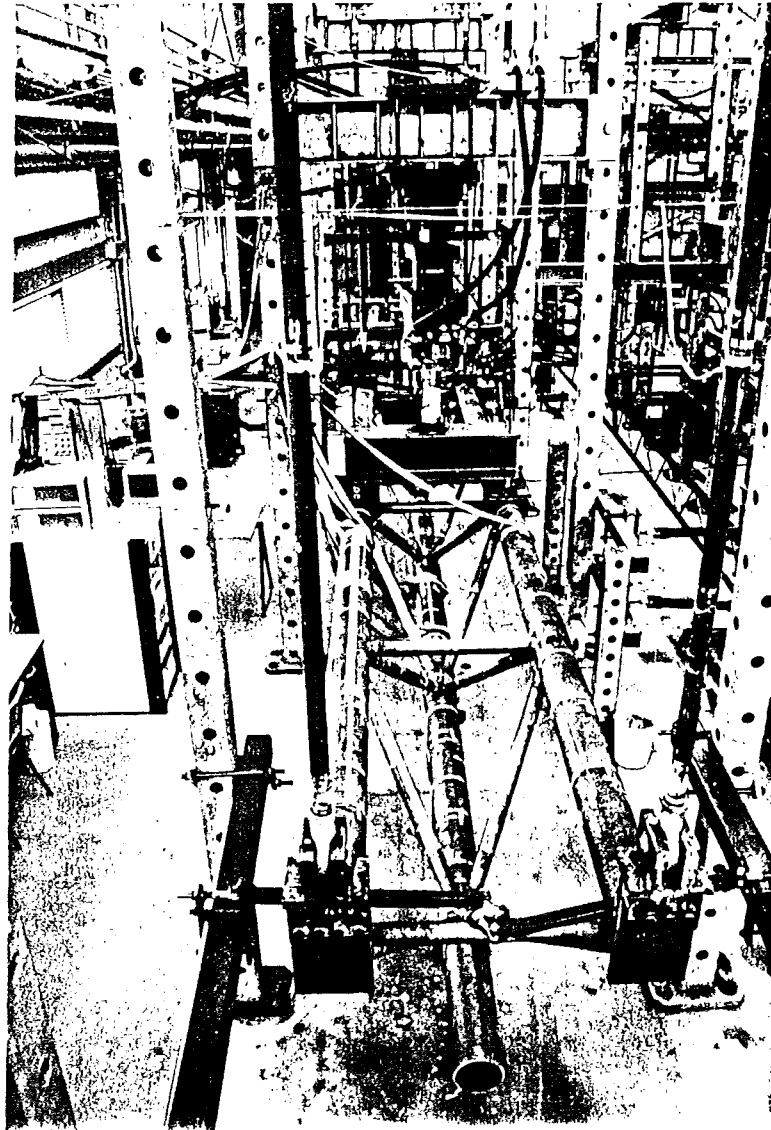


figure 3.1-4



Fig. 3.2.1 : Test rig for multiplanar test specimen in R.H.S.

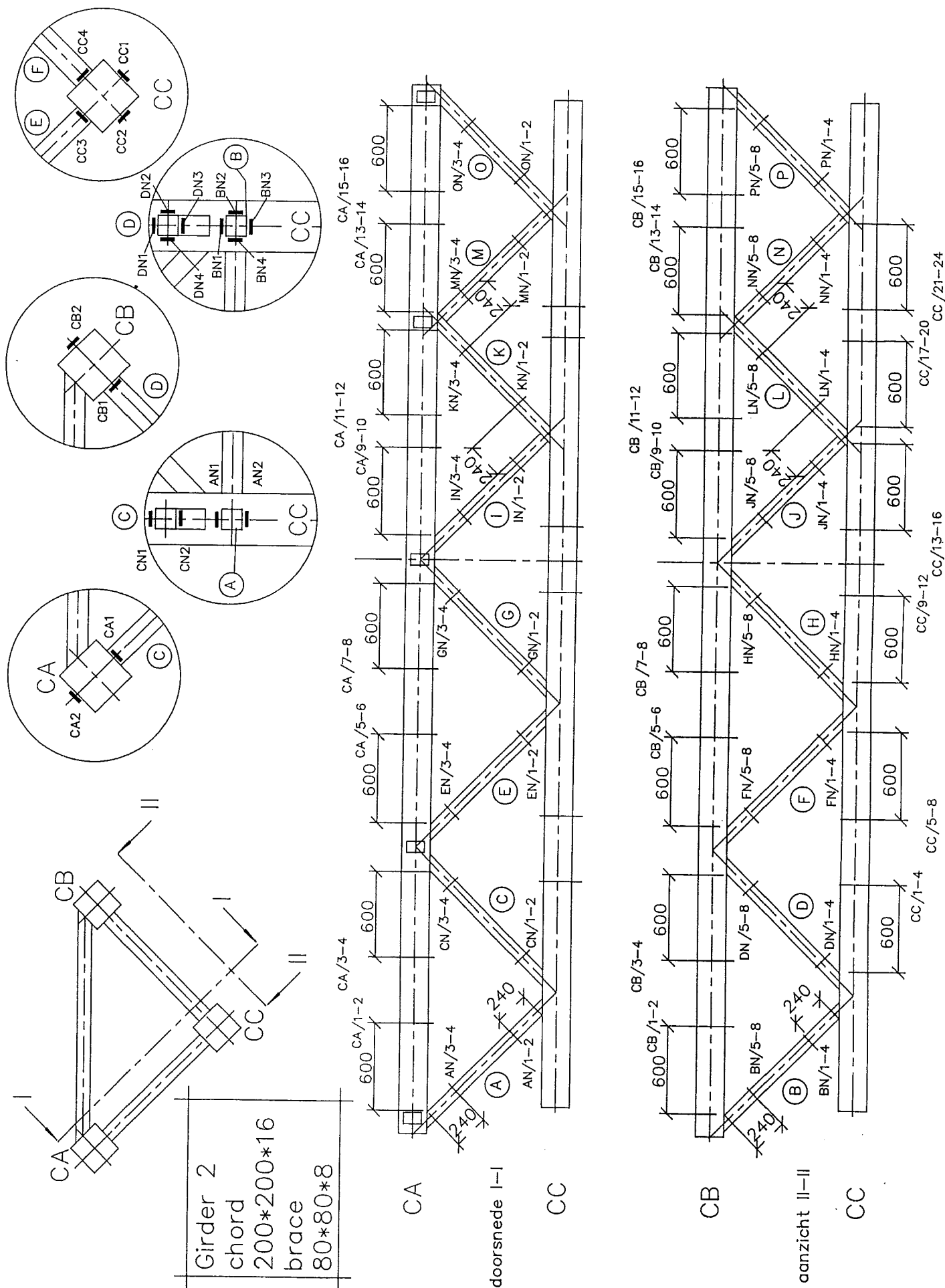


Fig. 3.2.2 : Locations of the strain gauges for determination of the bending moments and axial stresses (girder 2)

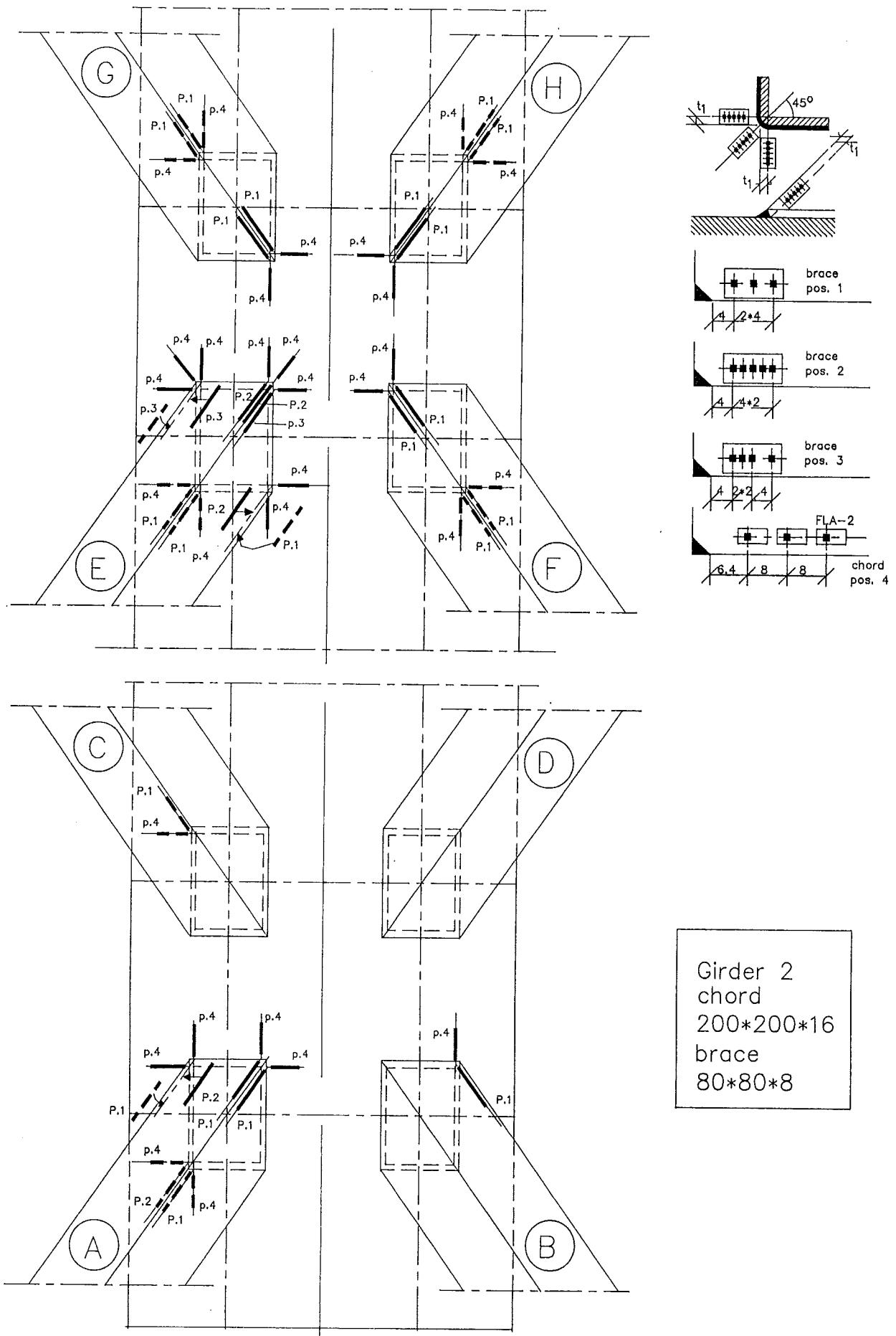
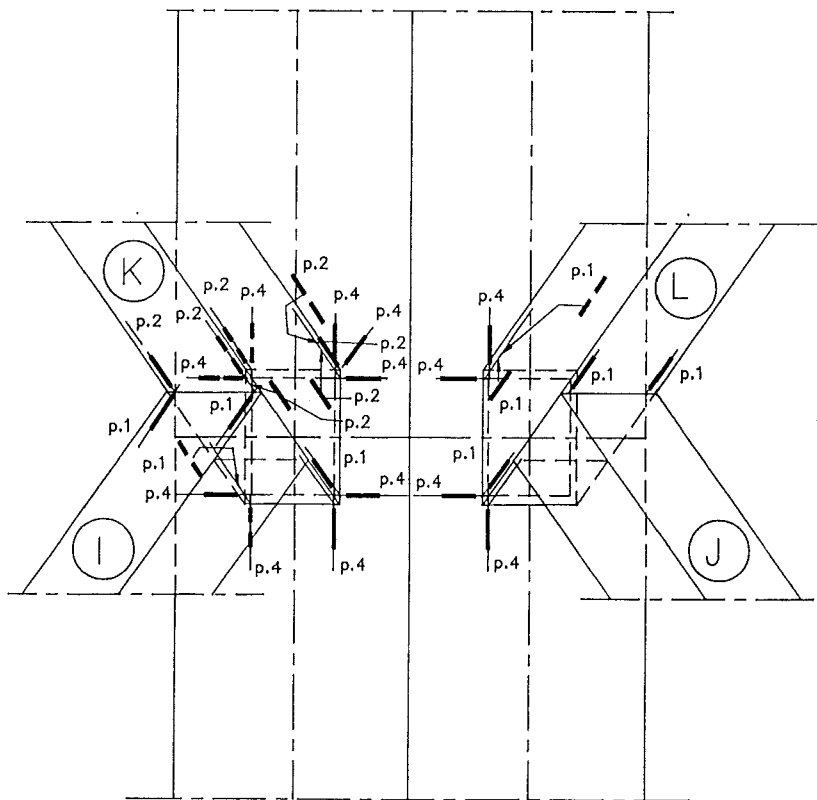
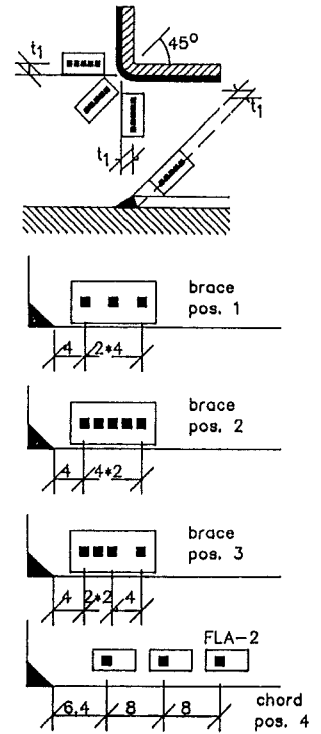
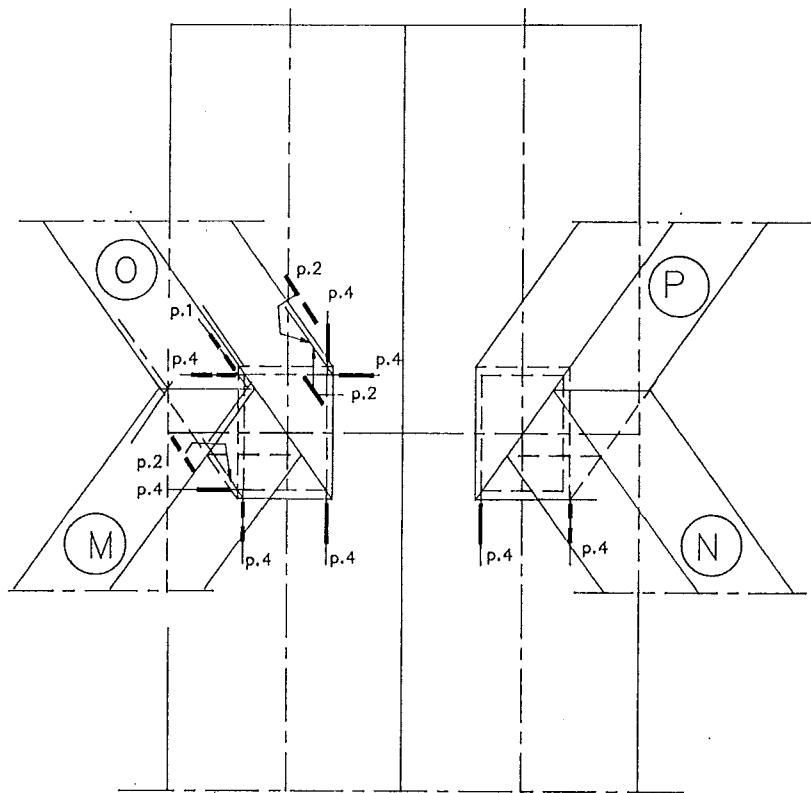
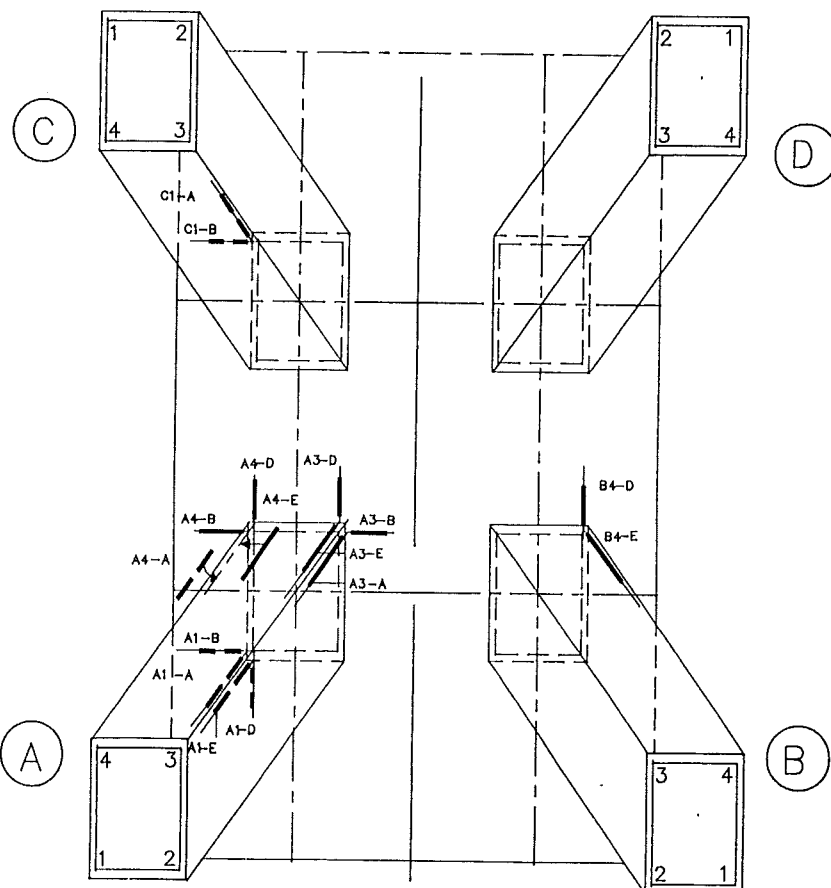
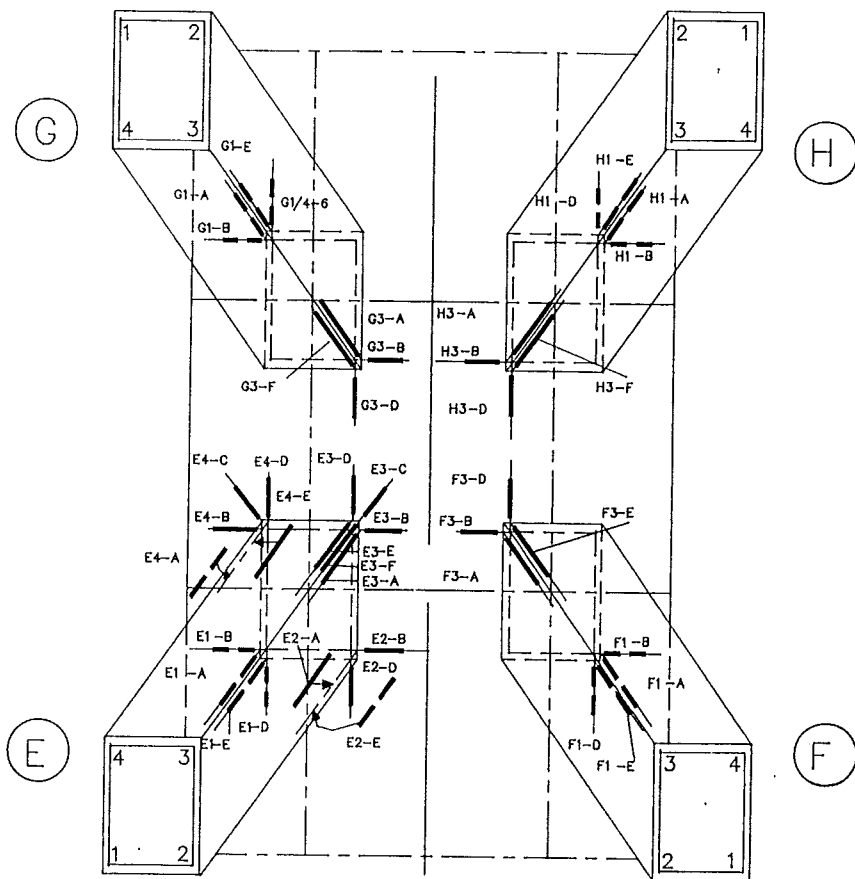


Fig. 3.2.3 : Position of the strain gauges of the joints with gap (girder 2)



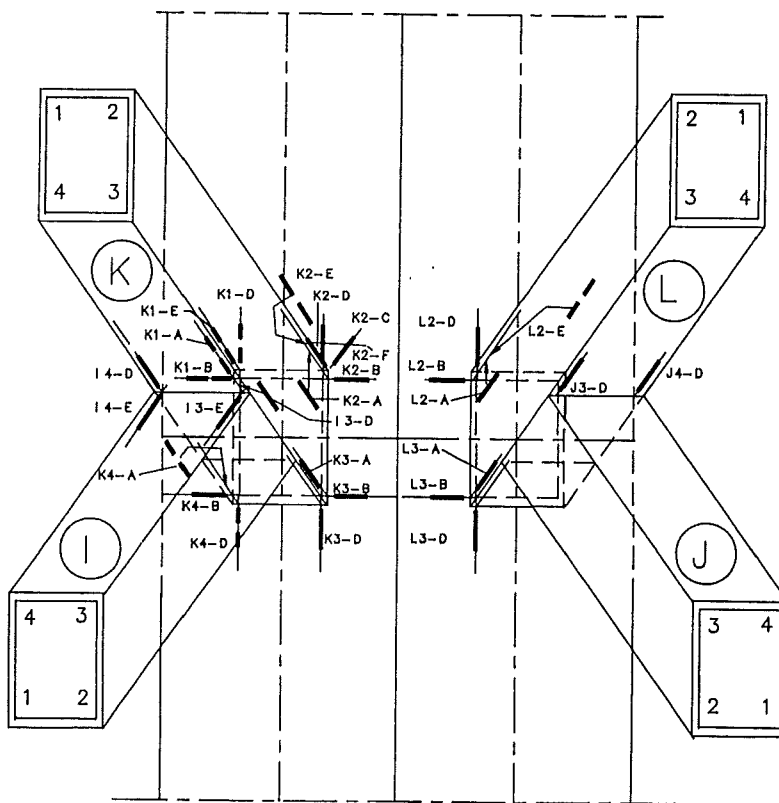
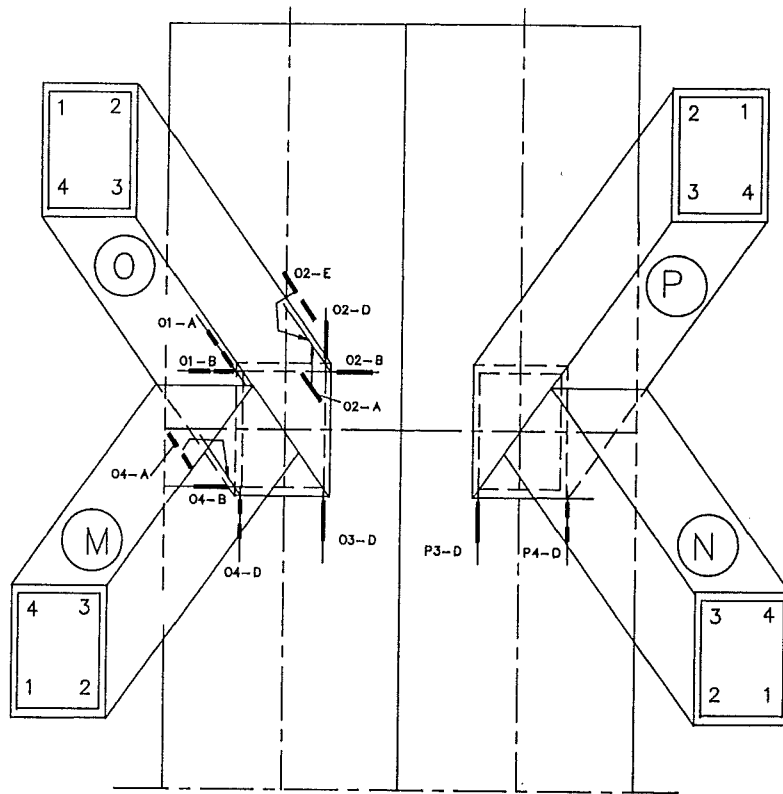
Girder 2  
 chord  
 200\*200\*16  
 brace  
 80\*80\*8

Fig. 3.2.4 : Position of the strain gauges of the overlapped joints (girder 2)



Girder 2  
 chord  
 200\*200\*16  
 brace  
 80\*80\*8

Fig. 3.2.5 : Numbering of locations of the joints with gap (girder 2)



Girder 2  
 chord  
 200\*200\*16  
 brace  
 80\*80\*8

Fig. 3.2.6 : Numbering of locations of the overlapped joints (girder 2)

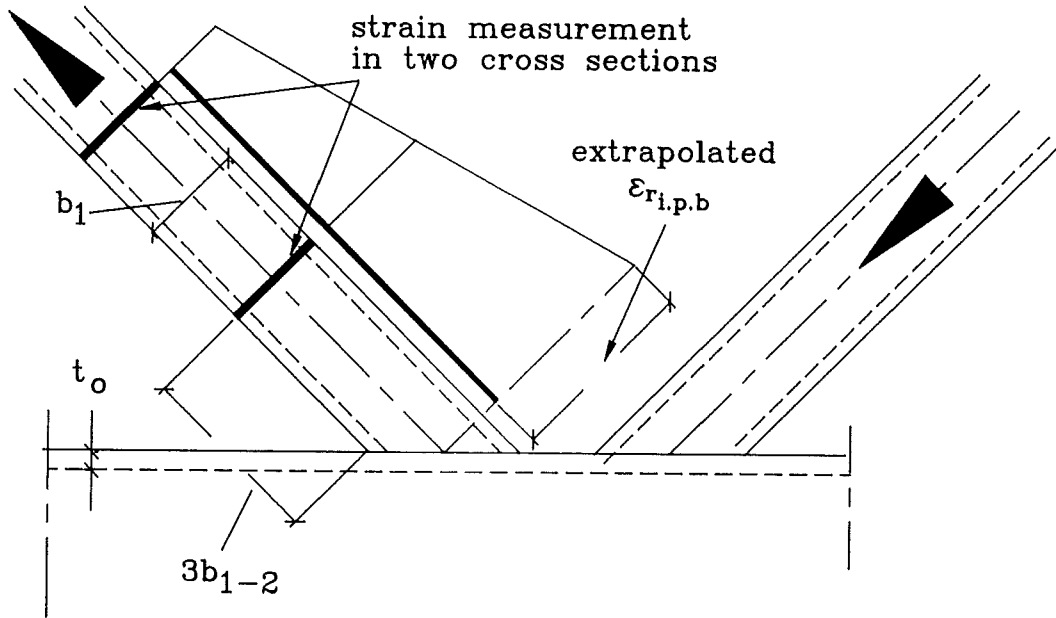
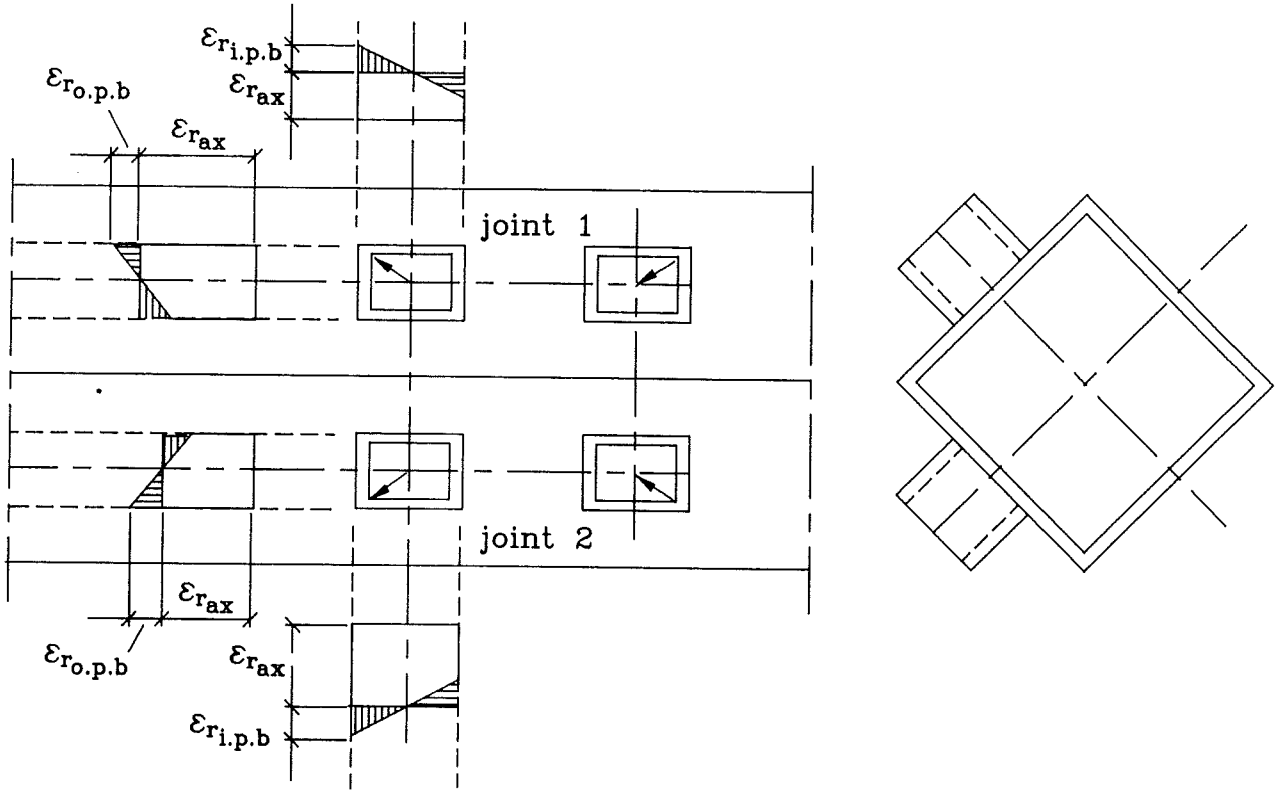
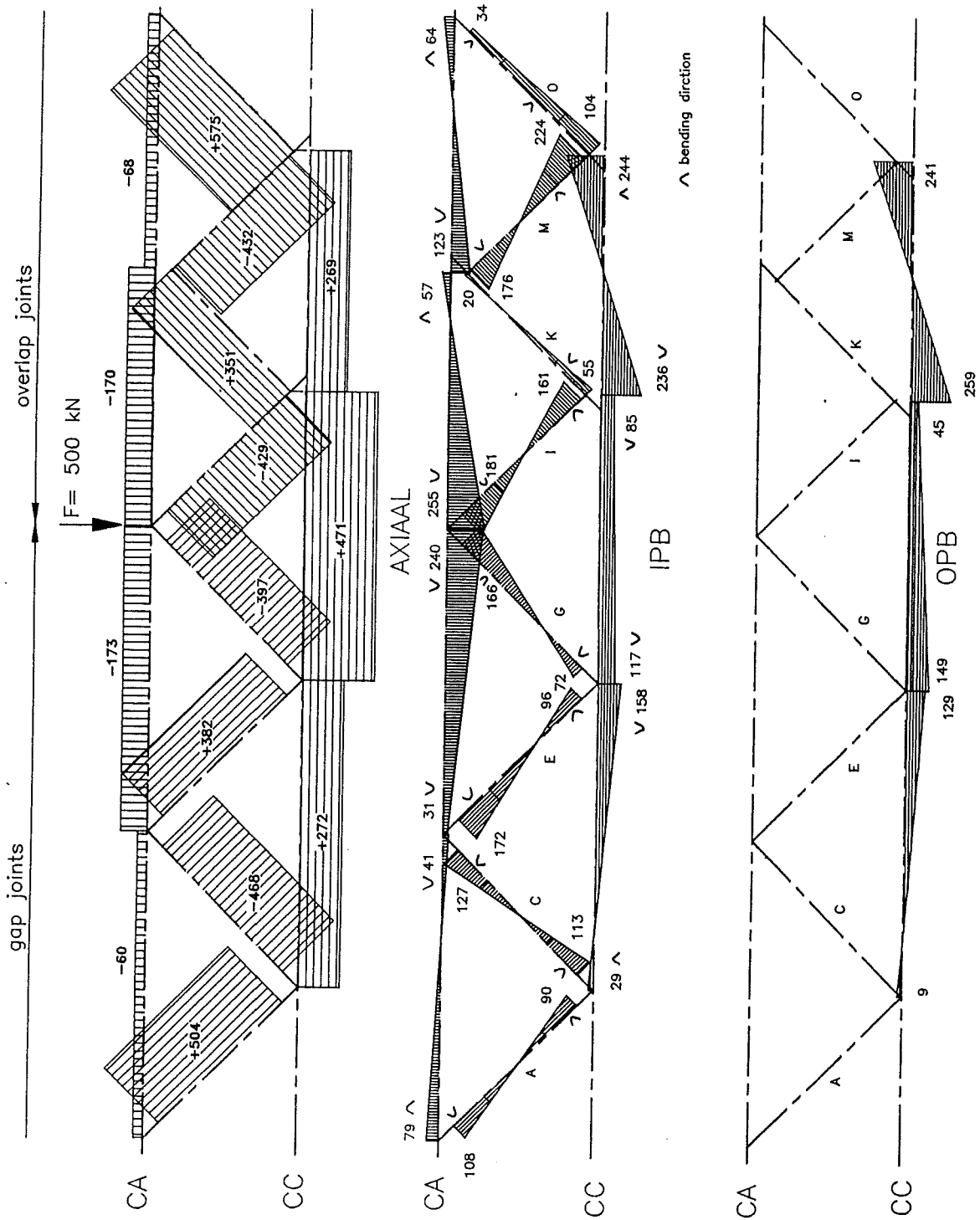
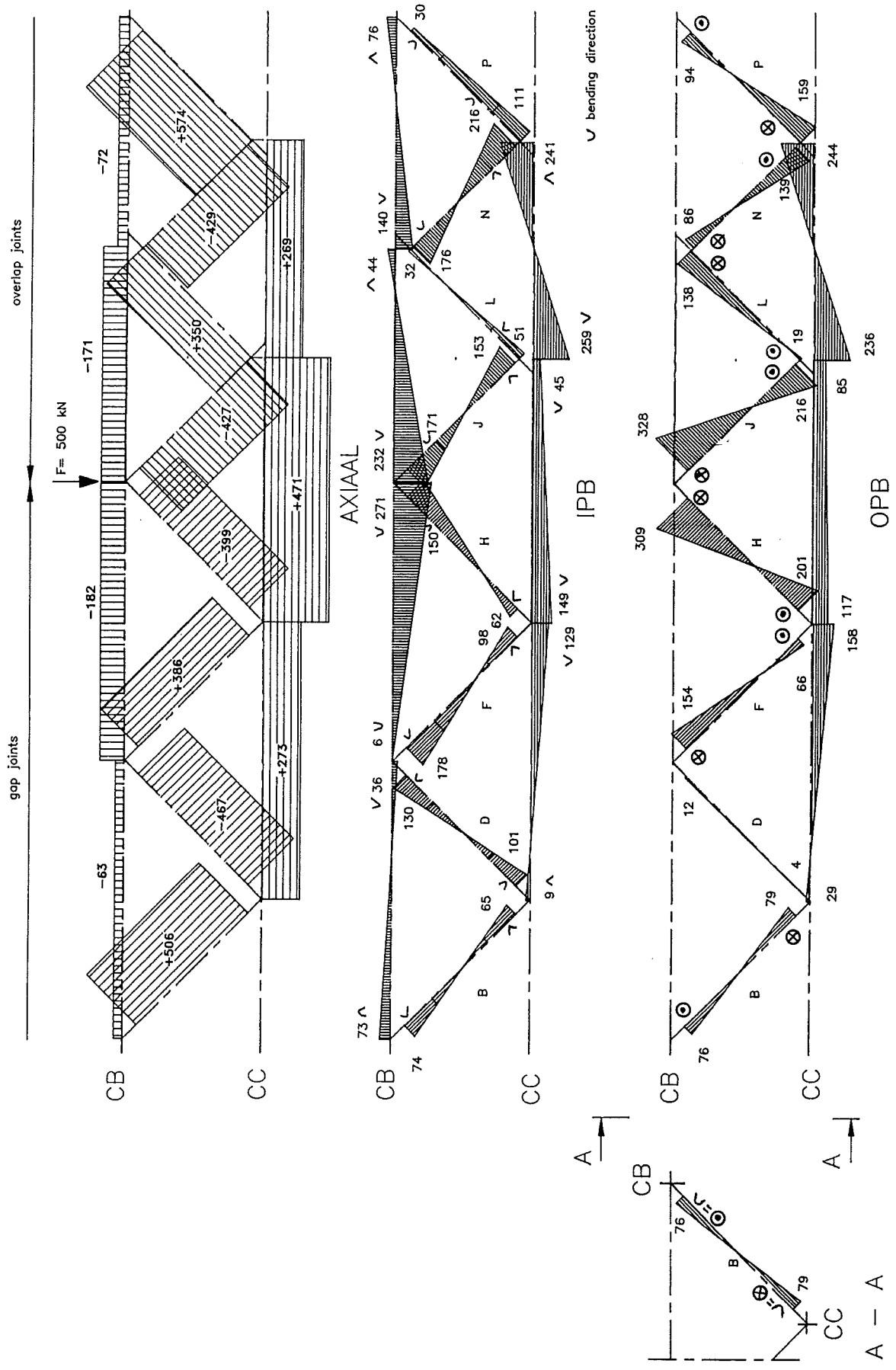


Fig. 3.2.7 : Determination of the bending strain at the intersection between brace and chord



On the braces in plane CC-CA no strain gauges available for measuring the out of plane bending

Fig. 3.2.8 : Nominal strain distribution due to axial loading and bending moments in Girder 2 (side CA-CC)



For statement of the symbols for out of plane bending direction see detail A-A (example brace B)

Fig. 3.2.9 : Nominal strain distribution due to axial loading and bending moments in Girder 2 (side CB-CC)

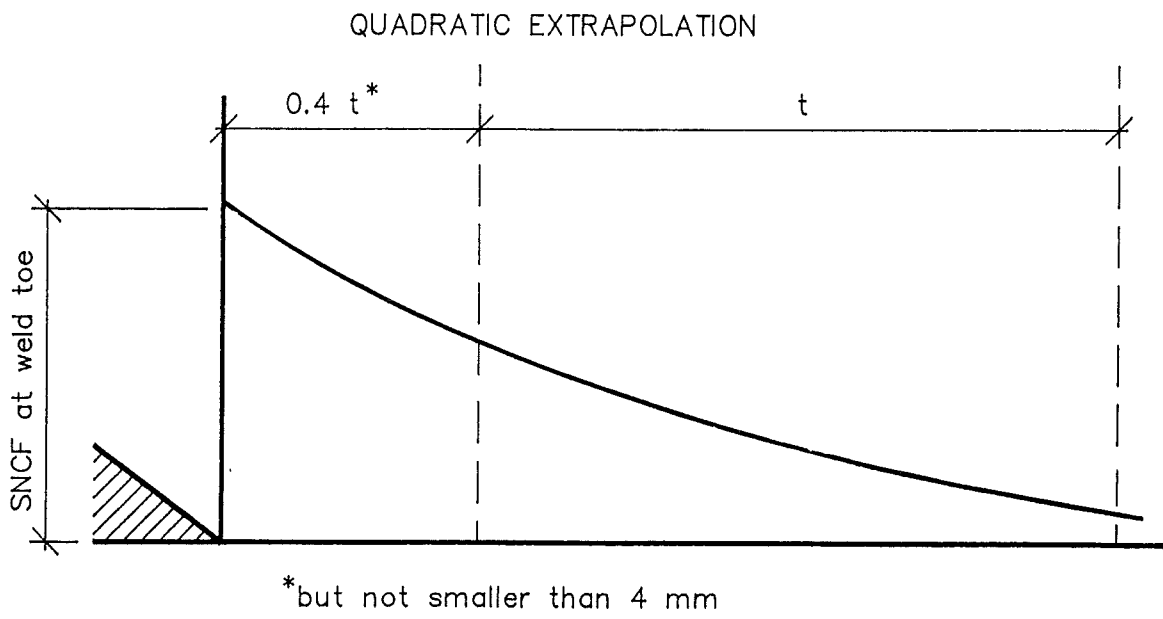


Fig. 3.2.10 : Method of quadratic extrapolation

NUMBERING OF THE CORNERS

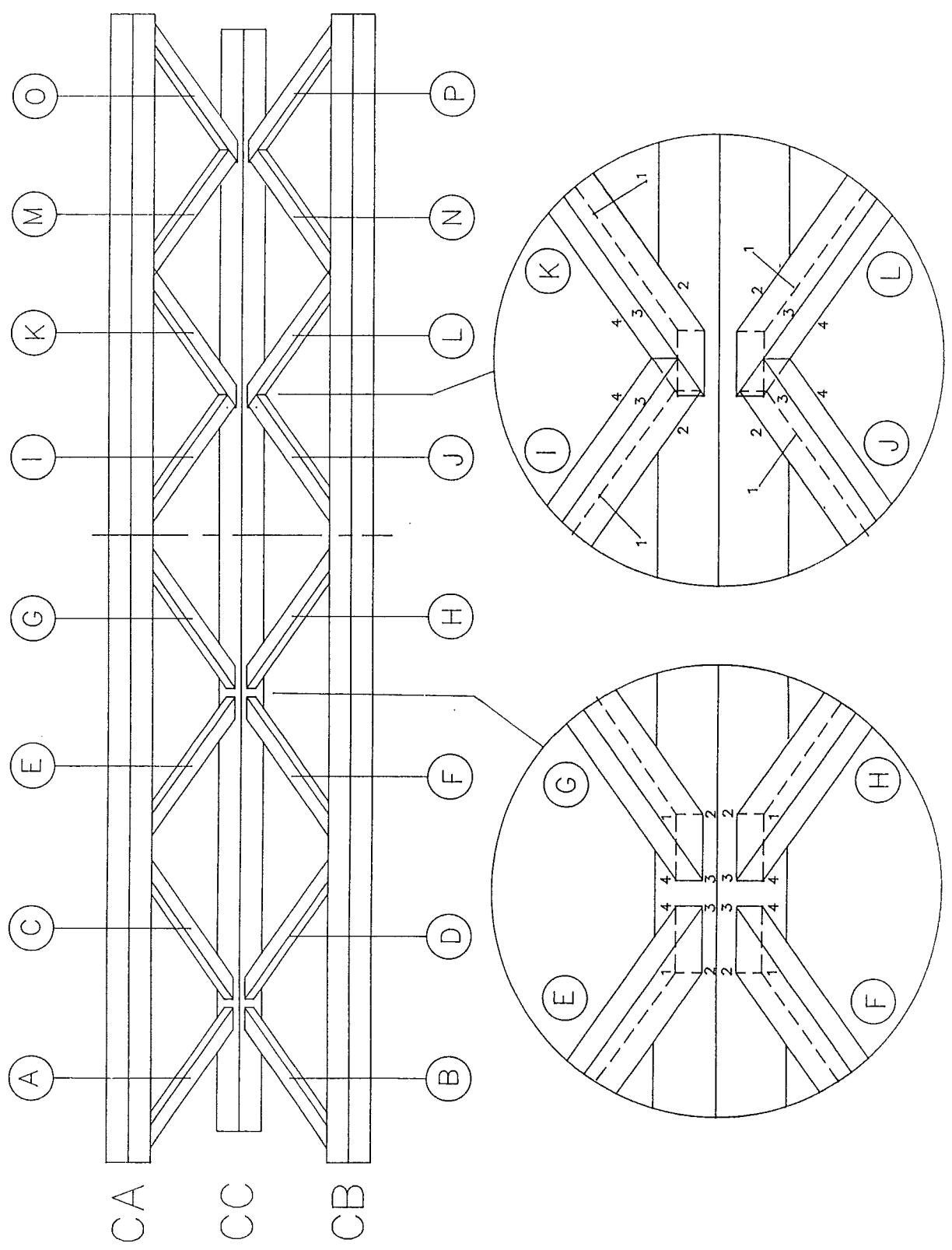
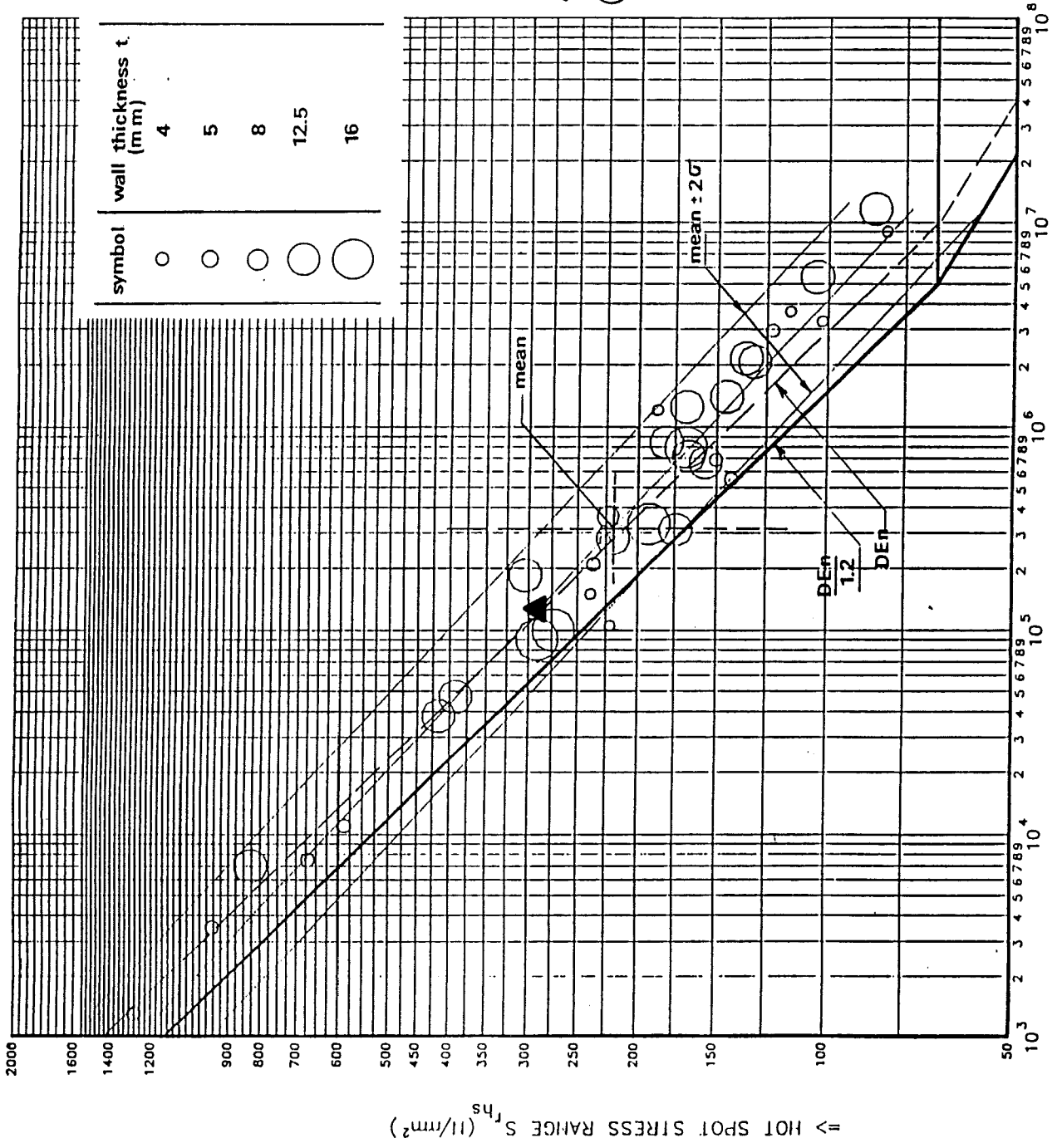


Fig. 3.2.11 : Girder 2, location of the members and numbering of the corners



Fig. 3.2.12 : Typical crack shape of an overlap joint, brace A of Girder 2



=> NUMBER OF CYCLES TO FAILURE  $N_f$   
CORRECTION OF ALL DATA BY  $(T/16)^{0.110} \log(N_f)$

Fig. 3.2.13 : Comparison of the fatigue results with the fatigue data derived from previous tests.